www.ietdl.org

Published in IET Communications
Received on 9th September 2013
Revised on 4th December 2013
Accepted on 19th December 2013
doi: 10.1049/iet-com.2013.0805

ISSN 1751-8628

Performance assessment of a wideband code-division multiple access-based radio-over-fibre system with near–far effect: downlink scenario

Gholamreza Baghersalimi

Department of Electrical Engineering, University of Guilan, P.O. Box 3756, Rasht, Iran
E-mail: bsalimi@guilan.ac.ir

Abstract: The impact of a radio-over-fibre subsystem on the total degradation (TD) performance of downlink wideband code-division multiple access with near–far effect is evaluated. The study investigates the use of pilot-aided channel estimation to compensate for the optical subsystem non-linearities for different channel conditions, estimation intervals, load factors (LFs) and near–far factors (NFFs). The results show that pilot-aided channel estimation is an effective method for compensating the composite impairments of the optical subsystem and the radio frequency channel. It is found that there is always a suitable quiescent point that optimises the system performance regardless of aforementioned conditions, however, the optimum achievable performance depends on the LF, spreading factor (SF) and NFF. Also, LF has more impact on the system performance in comparison to SF. Further, the optimum TD performance is only slightly affected by a decrease in the estimation interval over the optimum output backoff range.

1 Introduction

Radio-over-fibre (RoF) is a technology by which information-bearing signals using radio frequency (RF) carriers are distributed by means of optical components and techniques. Better coverage and increased capacity, centralised upgrading and adaptation, higher reliability and lower maintenance costs, support for future broadband applications and economic access to mobile broadband are among the most important advantages of RoF [1]. However, RoF systems are vulnerable to non-linearities in the optical subsystem that cause degradation of the system performance. The main areas of research in RoF include microwave and millimetre-wave RoF [2–4], RoF-based wireless local area networks (WLANs) [5, 6], RoF-based cellular systems [7], subcarrier multiplexed RoF systems [6], RoF-based wavelength division multiplexing [7] and RoF-based photonic code-division multiple access (CDMA) [8]. In particular, the estimation methods, modelling the radio subsystem, modelling the optical subsystem and multiple access techniques are regarded as the most important investigation topics in this context.

Channel estimation is a subject which has received a great deal of attention by researchers in recent years. In wireless systems, channel estimation techniques are used for the estimation of RF channel impulse response (CIR) in order to compensate for the amplitude distortion and phase rotation introduced by the RF channel variations. In cellular communication, estimation is achieved by time-multiplexed pilot signals, code-multiplexed pilot signals or a combination of these signals. In the wireless local area network (LAN) systems, on the other hand, estimation is carried out by frequency (subcarrier) multiplexed pilot signals, time (symbol) multiplexed pilot signals or a combination of these signals [9]. All such equalisation techniques require extra hardware at either the transmit and/or the receive side of the communication link.

In wideband code-division multiple access (WCDMA) systems, perfect power control that assumes all users have equal power is a very optimistic situation. An important issue in such systems is the near–far effect that arises when the channel gain between a user's transmitter and the receiver is different for different users [10]. In other words, the impact of an unequal transmit/receive power is relevant to a case where imperfect power control would give rise to the near–far problem. Typically, this configuration corresponds to the worst-case propagation scenario of all users being deployed in the cell. In a practical WCDMA cellular system, both the transmit power and spreading factor (SF) for each user would be selected to meet a target signal-to-interference plus noise ratio (SINR) and quality of service (QoS) subject to a maximum total transmit power constraint at the base station which leads to a range of transmit powers between users. This problem is particularly important in RoF systems (as a consequence of the non-linear behaviour) where any misalignment in transmit/receive power results in more distortion and hence different qualities for different users.

For RoF-based wireless communications, there is a dearth of publications in the context of channel estimation and compensation [1–6, 11–13]. In particular, for more realistic conditions, the collective effects of modulation, multiuser

© The Institution of Engineering and Technology 2014

interference (MUI), large signal distortion, data rate, near–far effect, load condition and estimation level have not been substantially investigated before.

It should be emphasised that both the amplitude and phase distortions of an optical channel affect the system performance. Also, due to the hysteresis-type memory of the optical subsystem, the entire RoF link suffers more from the phase impairments and frequency-dependent non-linearities when compared to a non-linear element such as RF high-power amplifier (HPA) as used in cellular mobile or satellite communications.

In this paper, the impact of the optical subsystem non-linearities on the performance of a downlink WCDMA cellular mobile system is studied with respect to the channel estimation and equalisation functions. The results for the WCDMA system total degradation (TD) performance are presented for different load factors (LFs), SFs, user numbers and estimation intervals when a code-multiplexed common pilot channel (CPICH) is used to compensate for the distortion introduced by both the optical channel and the RF channel. Strictly speaking, the overall subsystem that is, the optical (non-linear) subsystem and the RF channel (represented by AWGN – additive white Gaussian noise – and the near–far effect) is linearly estimated and equalised using CPICH under different conditions. Also, as this research focuses only on the optical subsystem, other sources of non-linearity, such as the RF HPA, are not considered. Further, for the sake of simplicity and focusing on the equalisation of the non-linear subsystem, operations such as coding and interleaving along with fading channel are not considered.

The paper is organised as follows: Section 2 introduces the theoretical background for estimating and equalising the optical subsystem. Section 3 presents the computer simulation model, while Section 4 presents the significant results and discussion of results. Finally, Section 5 concludes the paper.

2 System model and analysis

In this section, the mathematical background of the baseband downlink RoF-WCDMA model, which is shown in Fig. 1, is described. In general, this model comprises a transmitter, an optical link, an RF channel and a receiver. These subsystems are described in the following subsections.

2.1 Transmitter

Each user in the RoF-WCDMA system independently sends its data bit stream to the modulator where they are converted to a symbol train using the quadrature phase shift keying mapping rule. Let the kth user signal over the frame period T_{fr} be denoted by

$$x_k(t) = \sum_{n=1}^{N_s} X_{k,n}\delta(t-(n-1)T_s); \quad 0 \le t \le T_{\text{fr}} \qquad (1)$$

where $X_{k,\,n} = b_{k,n} + jd_{k,n}$ is the nth symbol of the kth user, $b_{k,n}$ is the nth symbol's in-phase component of the kth user, $d_{k,n}$ is the nth symbol's quadrature component of the kth user, T_s is the symbol period for all users, N_s is the number of data

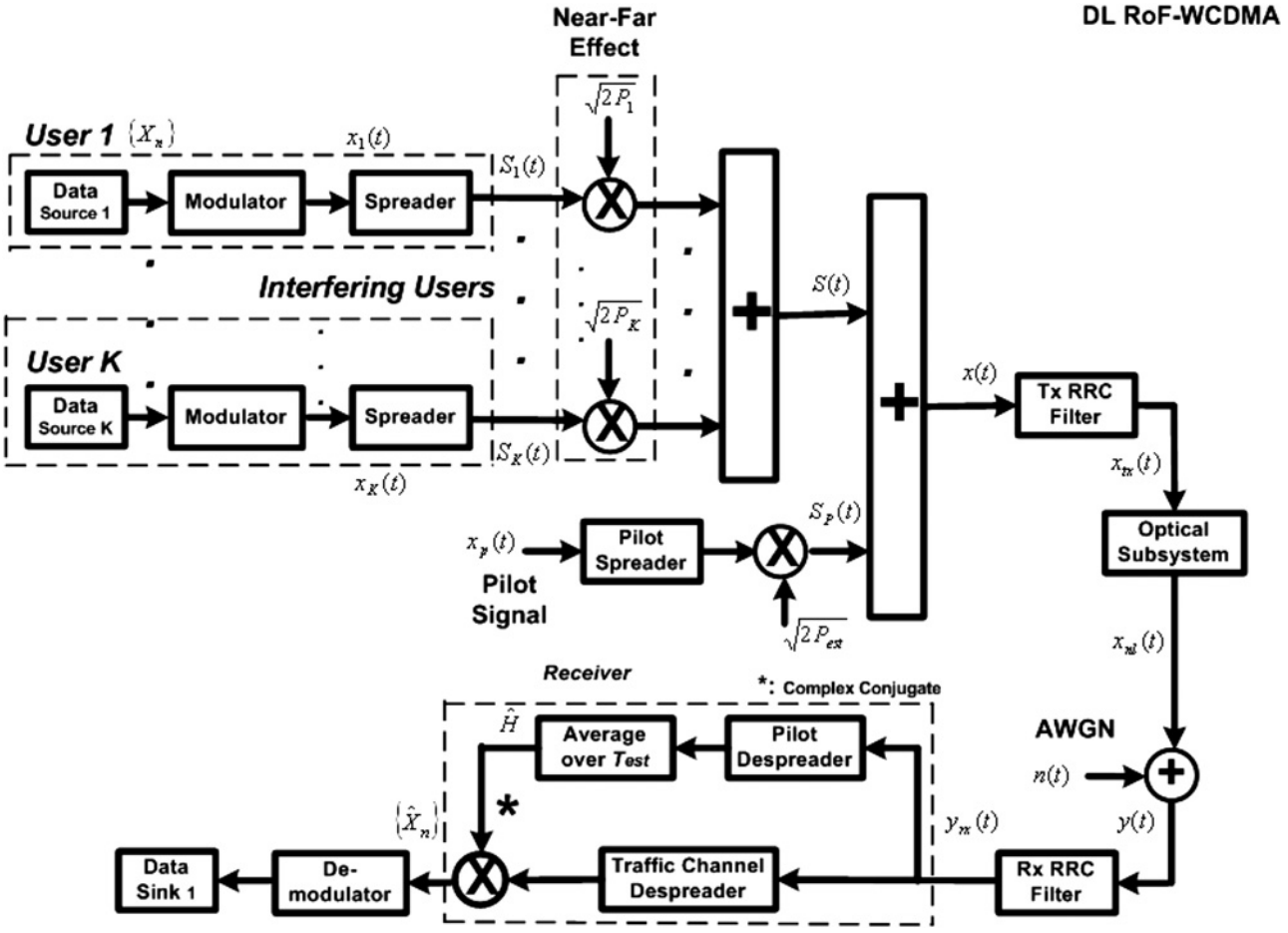

Fig. 1 *Downlink RoF-WCDMA system model*

© The Institution of Engineering and Technology 2014

symbols being transmitted for each user in the frame period $T_{fr} = N_s T_s$, and $\delta(t)$ is the Dirac delta function. In the above relationship, it is assumed that all users transmit at the same data rate, or equivalently, have the same spreading factor. Without loss of generality, in order to simplify the notation it is assumed that the first user is the intended user, so that the intended user's signal over the frame period ($0 \le t \le T_{fr}$), with unit power, can be written without the index $k = 1$ as shown in (2).

$$x_1(t) = \sum_{n=1}^{N_s} X_n \delta(t - (n-1)T_s) = \sum_{n=1}^{N_s} (b_n + jd_n)\delta(t - (n-1)T_s) \tag{2}$$

Each information-bearing signal is then multiplied by the corresponding spreading sequence, as described by (3)

$$g_k(t) = \sum_{m=1}^{SF} c_{k,m}\delta(t - (m-1)T_{ch}); \quad 0 \le t \le T_s \tag{3}$$

where SF is the data spreading factor which is assumed to be the same for all users, T_{ch} is the chip duration and $c_{k,m}$: $m = 1, 2, \ldots,$ SF is the mth element (chip) of the kth user's binary spreading sequence. The spreading sequences are chosen from the Walsh-Hadamard (WH) sequences which are mutually orthogonal [14]. In addition, if the spreading signal of the kth user over a whole frame interval is denoted by (4)

$$\begin{aligned} z_k(t) &= \sum_{n=1}^{N_s}\sum_{m=1}^{SF} c_{k,m}\delta(t - (n-1)T_s - (m-1)T_{ch}) \\ &= \sum_{n=1}^{N_s} g_k(t - (n-1)T_s); \quad 0 \le t \le T_{fr} \end{aligned} \tag{4}$$

then the kth user spread signal of average power P_k and the total multiuser spread signal over the same frame interval can be represented, respectively, by (5) and (6)

$$S_k(t) = \sum_{n=1}^{N_s} X_{k,n} g_k(t - (n-1)T_s) \tag{5}$$

$$S(t) = \sum_{k=1}^{K}\sum_{n=1}^{N_s} \sqrt{2P_k}[X_{k,n} g_k(t - (n-1)T_s)] \tag{6}$$

where K is the total number of users. Then, the CPICH is added to the transmitted signal in order to provide a channel estimation mechanism. The spreading sequence of this signal is defined by (7)

$$g_p(t) = \sum_{i=1}^{SF_p} q_i \delta(t - (i-1)T_{ch}); \quad 0 \le t \le T_p \tag{7}$$

where SF_p is the spreading factor of the pilot signal, q_i: $i = 1, 2, \ldots, SF_p$ is the ith element of the spreading sequence of the pilot signal and T_p is the duration of a pilot symbol. Also, the transmit pilot symbol sequence (i.e. the non-spread pilot signal) can be represented by (8)

$$x_p(t) = \sum_{j=1}^{N_p} a_j \delta(t - (j-1)T_p); \quad 0 \le t \le T_{fr} \tag{8}$$

where a_j is the jth transmit pilot symbol and N_p is the number of pilot symbols per frame, hence $T_{fr} = N_p T_p$. Therefore, the spread pilot signal over a frame time, which is known to the receiver, can be described by (9).

$$S_p(t) = \sum_{j=1}^{N_p} a_j g_p(t - (j-1)T_p); \quad 0 \le t \le T_{fr} \tag{9}$$

Hence, the total transmit signal over a frame is given by

$$x(t) = \sum_{k=1}^{K}\sum_{n=1}^{N_s} \sqrt{2P_k}[X_{k,n} g_k(t - (n-1)T_s)] + \sqrt{2P_{est}} S_p(t) \tag{10}$$

where P_{est} is the average power of the pilot signal.

To consider the near–far effect, it is assumed that the amplitude of the received/transmitted signal varies over the interval $[1-\eta,\ 1+\eta]$, where $\sqrt{2P_1} = (1-\eta)$ corresponds to the furthest user (mobile unit) and $\sqrt{2P_K} = (1+\eta)$ corresponds to the nearest user [15]. Clearly, $\eta = 0$ corresponds to a case where there is no near–far problem. In this paper, it is assumed that the amplitude variation (at either the transmitter or the receiver) is linearly changed over the aforementioned interval, hence the near–far effect is considered by taking the amplitude of the kth user as (the average power of each user's symbols is assumed to be unity)

$$\begin{aligned} \sqrt{2P_k} &= (1-\eta) + \frac{2\eta}{(K-1)}(k-1); \quad k \\ &= 1, 2, \ldots, K \end{aligned} \tag{11}$$

Also, the near–far factor (NFF) is defined by

$$\mathrm{NFF} = 10\log\frac{\min p_i}{\max p_i} = 20\log\frac{(1-\eta)}{(1+\eta)} \tag{12}$$

where min p_i and max p_i are the minimum and maximum transmit/receive power of users [15]. The smaller the NFF, the more destructive the near–far effect. Also, the furthest user (with the minimum power) and the nearest user (with the maximum power) are denoted by $k = 1$ and $k = K$ (number of users), respectively. By defining parameter R as the ratio of the pilot power P_{est} to the total transmit power P_t as shown in (13)

$$R = \frac{P_{est}}{P_t} \tag{13}$$

then the total transmit power is given by

$$P_t = KP_u + P_{est} \tag{14}$$

where P_u is the average power of users $\left(P_u = \left(\sum_{k=1}^{K} P_k\right)/K\right)$

© The Institution of Engineering and Technology 2014

doi: 10.1049/iet-com.2013.0805

and the number of users K is given by (15).

$$K = \lfloor \mathrm{SF} \times \mathrm{LF} \times (1 - R) \rfloor \tag{15}$$

The term in $\lfloor x \rfloor$ denotes the largest integer not greater than x and LF denotes the cell load factor. The parameter LF determines the number of users in the system whereby increasing this factor, more users can use the same communication channel. However, the total transmit power is fixed thereby the power of each user increases as a result of decreasing LF or alternatively the number of users. The parameter R must be chosen in order to achieve reliable detection at the receiver without consuming excess resources within the cellular system. Subsequently, the resultant signal is up-sampled and filtered by the transmit root raised cosine (RRC) filter as shown in (16)

$$x_{\mathrm{tx}}(t) = h_{\mathrm{rrc}}(t) * x(t) \tag{16}$$

where * denotes convolution and $h_{\mathrm{rrc}}(t)$ denotes the impulse response of the RRC filter, with roll-off factor equal to 0.22 and oversampling factor equal to 4.

2.2 Optical subsystem

In the analysis of communication systems, analytic models of subsystems are preferred because they normally lead to closed-form analytic solutions for the system. However, these models are only valid under certain conditions and assumptions. In addition, some analytic techniques such as the Volterra series approach (for non-linear systems with memory such as the laser diode which is described by the rate equations) are very difficult to treat. Further, in some cases the physical problems cannot be represented by mathematical models. One alternative for describing such complex systems is behavioural modelling. In behavioural modelling, the system is treated as a black box with transfer characteristics described by a set of equations. For an optical system, the transfer characteristics are expressed as AM–AM (amplitude-to-amplitude) and AM–PM (amplitude-to-phase) characteristics (also known as the large-signal response). The black box model accounts for the composite effects of all impairments in the system such as static and dynamic non-linearities and optical noise. The main advantage of behavioural modelling is that it can describe a complex system without needing to have a detailed knowledge of its constituent subsystems or components.

The use of AM–AM/PM models is based on the underlying assumption that the envelope of the signal is varying slowly such that the model, rather than the instantaneous value of signal, is used. The models are valid when the device 'memory time' (amplitude- and frequency-dependent time delay between the transmitted and received RF signal) is much smaller than the reciprocal of the input signal bandwidth [16]. In other words, these characteristics can be used only when the non-linear system is treated as a quasi-memoryless system [17]. As a rule of thumb, the AM–AM/PM models are used when the memory of the non-linear system is at least twice less than the reciprocal of the envelope frequency [16, 18]. This condition is met in this study.

The optical subsystem used in this research comprises a laser diode (LD), a 2.2 km long single-mode fibre and a photodiode (PD) [11]. The optical transmitter used is a directly modulated InGaAsP distributed feedback (DFB) LD with an operating wavelength of 1310 nm. Also, the optical receiver consists of an overall 32 dB gain which completely compensates for the total loss of this optical link. The radio frequency is 1.8 GHz, although the frequency response of the link is flat over frequencies $1.7 < f < 2.2$ GHz. The AM–AM/PM transfer functions are shown in Fig. 2. Further, a pictorial description of output back-off

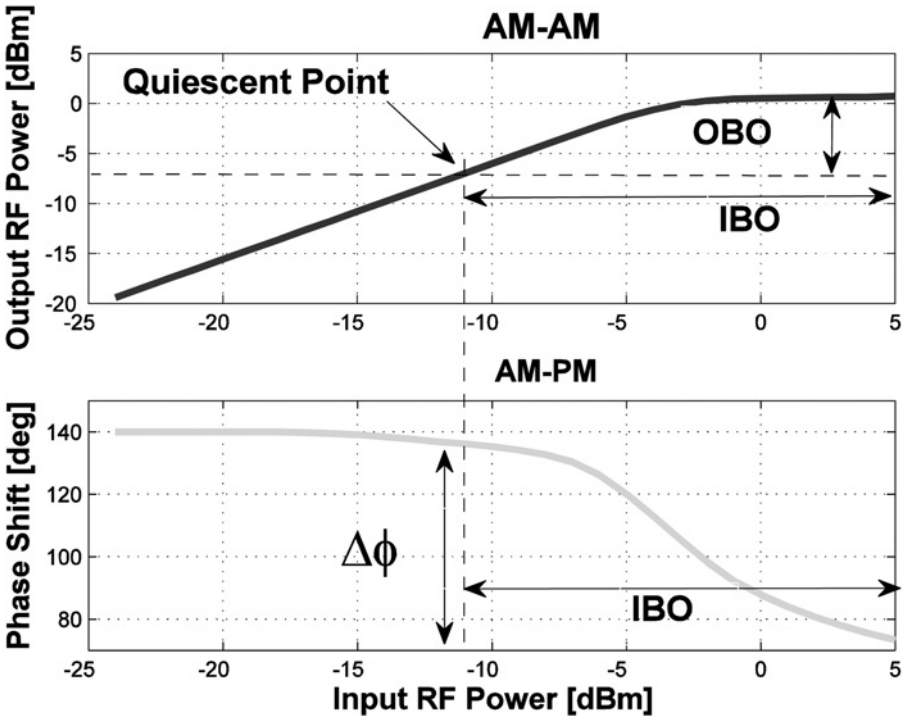

Fig. 2 *AM–AM/PM characteristics (IBO: input back-off) [13]*

© The Institution of Engineering and Technology 2014

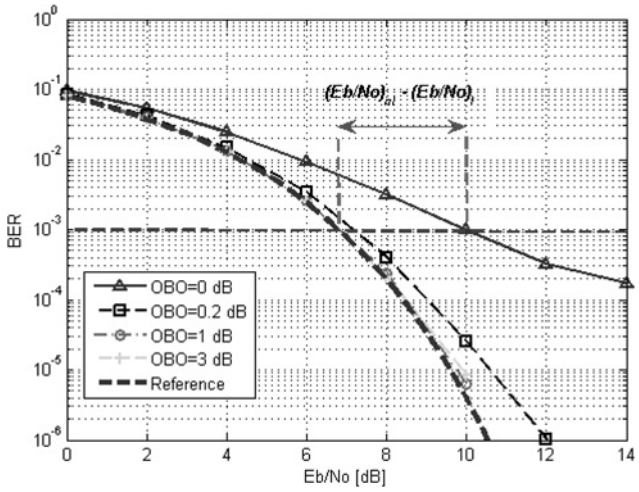

Fig. 3 *BER against E_b/N_0 for DL RoF-WCDMA with no near–far effect*

(OBO) is shown in Fig. 3 and is defined (on a logarithmic scale) as the difference between the maximum output power and the output power at the quiescent point.

The RRC filtered signal passes through the non-linear optical subsystem whose output is given by (17)

$$x_{\mathrm{nl}}(t) = G_{\mathrm{out}}\sqrt{\frac{2}{R_{\mathrm{out}}}f_{\mathrm{AM-AM}}(0.5R_{\mathrm{in}}(G_{\mathrm{in}}|x_{tx}(t)|)^2)} \times \exp\left[jf_{\mathrm{AM-PM}}(0.5R_{\mathrm{in}}(G_{\mathrm{in}}|x_{tx}(t)|)^2 + j\psi_{x_{tx}}(t)\right] \tag{17}$$

where $G_{\mathrm{in}} = \sqrt{(\max(P_{\mathrm{RF},i})/\mathrm{IBO} \times P_{\mathrm{m}})}$ is the gain of the pre-amplifier that matches the output power of the transmit RRC filter to the input power of the optical subsystem [11]; IBO is the input back-off on a linear scale, P_{m} is the maximum input RF power to the optical subsystem before the pre-amplifier, $\max(P_{\mathrm{RF},i})$ is the (measured) maximum input RF power before the pre-amplifier, $\psi_{x_{tx}}(t)$ is the phase of the signal $x_{tx}(t)$, $R_{\mathrm{in}} = 50\ \Omega$ is the input impedance of the optical subsystem, $R_{\mathrm{out}} = 50\ \Omega$ is the output impedance of the optical subsystem, and G_{out} is a linear gain which sets the overall gain of the optical subsystem to unity. Also, $f_{\mathrm{AM-AM}}(\cdot)$ and $f_{\mathrm{AM-PM}}(\cdot)$ are the AM–AM and AM–PM transfer function characteristics of the non-linear (optical) subsystem, respectively.

2.3 RF channel

Following the optical subsystem, the signal is perturbed by a zero-mean complex AWGN process $n(t)$. So, the received signal is represented by

$$y(t) = x_{\mathrm{nl}}(t) + n(t) \tag{18}$$

Also, (18) can be rewritten by using

$$x_{\mathrm{nl}}(t) = x_{\mathrm{s1}}(t) + n_{\mathrm{d}}(t) \tag{19}$$

where $x_{\mathrm{s1}}(t)$ is the up-sampled (and possibly amplified/attenuated) version of signal $S_1(t)$, and $n_{\mathrm{d}}(t)$ is the total distortion introduced by the near–far effect, optical subsystem and other users. Further, E_{b} is defined as the average bit energy of the intended user while the signals from other users are treated as an MUI. So, the received signal can be represented by (20).

$$y(t) = x_{\mathrm{s1}}(t) + n_{\mathrm{d}}(t) + n(t) \tag{20}$$

Then, the SINR is given by (21).

$$\mathrm{SINR} = \frac{E[x_{\mathrm{s1}}^2(t)]}{E[n_{\mathrm{d}}^2(t) + n^2(t)]} \tag{21}$$

2.4 Receiver

At the receiver, the noise perturbed signal is filtered by the receive RRC filter followed by down-sampling, where the output of this filter is given by (22).

$$y_{rx}(t) = h_{\mathrm{rrc}}(t) * y(t) \tag{22}$$

In this paper, the joint optical and RF (including AWGN and near–far effect) channels are estimated using a pilot symbol channel estimation technique. That is, pilot symbols are used to train sequences for estimating the combined optical and RF CIR.

In general, by using post-correlation compensation, all estimates are averaged over the estimation time T_{est} (which is shorter than T_{fr}) according to a strategy to give a complex estimate for that particular interval. Then all estimates are applied to the data signal in the corresponding time intervals. This process is repeated for all time intervals per frame. For example, in [14] a multi-slot (each slot corresponds to 1/15th of a frame duration) moving window averaging (MWA) filter was used to determine the final channel estimate in a particular slot. Thereafter, each final estimate per slot was used to compensate for the channel impairment in the corresponding data slot. As another example, a six-symbol MWA filter was used in [19] to obtain the final channel estimate per symbol. Then, each final estimate per symbol was applied to the corresponding data symbol.

In this paper, a channel estimate is obtained during the interval T_{est}, and then applied to the whole frame. In other words, after deriving the channel estimate, it is immediately applied to the entire data frame. This approach reduces the processing time and complexity of the receiver. The estimate extraction process comprises two vector multiplications (i.e. the pilot spreading code and transmit pilot) followed by an integration over T_{est}. The shorter the estimation time, the shorter the length of the two vectors, hence a more time-efficient process can be achieved. Nonetheless, averaging over longer periods gives better estimates of the channel. This concept is investigated using TD as the main metric for different estimation durations, including frame, slot and symbol periods. The estimated channel (optical subsystem + near–far effect) transfer function can be represented by (23).

$$\hat{H} = \int_0^{T_{\mathrm{est}}} y_{rx}(t)S_p(t)^*\mathrm{d}t \tag{23}$$

Therefore, the nth received symbol for intended user-1 in the time interval $(n-1)T_{\mathrm{s}} \le t \le nT_{\mathrm{s}}$, as denoted by $\hat{X}_n$, may be

© The Institution of Engineering and Technology 2014

doi: 10.1049/iet-com.2013.0805

represented by (24).

$$\hat{X}_n = \hat{H}^* \int_{(n-1)T_s}^{nT_s} y_{rx}(t) Z_1(t)\, \mathrm{d}t = \hat{b}_n + j\hat{d}_n \qquad (24)$$

The term $Z_1(t)$ denotes the spreading waveform of user-1 while the terms in $\hat{b}_n$ and $\hat{d}_n$ are the in-phase and quadrature components, respectively, of user-1's nth estimated symbol, that is, $\hat{X}_n$. The data bits are then collected at the data sink and compared to those transmitted.

It should be emphasised that the value of the proposed estimation method compared with previous studies in the literature is that by using the existing channel estimation and correction techniques, the distortion due to the optical subsystem can be accommodated without using extra hardware at either the transmit and/or the receive side of the communication link. Also, the comprehensive nature of the study, which models the collective effects of the modulation, MUI, large signal distortion, estimation interval, SF, LF and near–far effect as well as channel estimation and equalisation, contributes to the unique value of the work undertaken.

3 Simulation setup

To evaluate the effects of the optical subsystem on WCDMA in the presence of near–far effect, computer simulations were carried out based on the system model presented in Fig. 1. A key performance metric for non-linear systems is the TD, which is defined as [20]

$$\mathrm{TD}\ [\mathrm{dB}] = (E_b/N_0)_{\mathrm{nl}} - (E_b/N_0)_{\mathrm{l}} + \mathrm{OBO} \qquad (25)$$

where $(E_b/N_0)_{\mathrm{nl}}$ and $(E_b/N_0)_{\mathrm{l}}$ are the required (E_b/N_0) for the non-linear system and the linear system, respectively, at a target bit error rate (BER). The small value of OBO means that the quiescent point of the non-linear system (optical subsystem) is near saturation, for which a high efficiency is achieved; however, the output signal will be highly distorted. Hence, a higher (E_b/N_0) is needed to compensate for this effect compared to the linear case. For large values of OBO, the optical subsystem works in the linear region, so there will be minimal distortion. The loss of subsystem efficiency through the use of high OBO values is taken into account in the TD expression. So, by increasing the OBO value, it is reasonable to expect an optimum value for the OBO that minimises the TD. In other words, one main goal of this research is to determine the optimum OBO that minimises (25).

To enable statistically valid simulation results in reasonable simulation times, Monte-Carlo methods are used during the simulation at target BER = 10^{-3}. Also, the WCDMA system parameters [21, 22] and optical subsystem parameters [11] are summarised in Tables 1 and 2, respectively.

Table 1 WCDMA system parameters

Quantity	Value
frame length	10 ms
spreading factor (SF)	data: 32, 64, 68; pilot: 256
data rate	120 kbps (SF = 64)
load factor (LF)	25%, 50%, 75%, 100%
near–far factor (NFF)	0, −1, −3 dB
amplitude variation η	0, 0.0575, 0.171
number of frames	800
chip rate	3.84 Mcps
estimation level, T_{est}	frame: 10 ms slot: 0.667 ms symbol: 0.0167 ms
ratio of pilot power to total power R	10%
target BER	10^{-3}
confidence interval	95%

Table 2 Optical subsystem parameters

Quantity	Value
output back-off	0–3 dB
max($P_{\mathrm{RF},i}$) [ref. value for OBO]	3.1623 mW (≡ 5 dBm)
wavelength	1310 +/– 10 nm
modulation gain	0.12 mW/mA
PD responsivity	0.75 mA/mW
fibre type	single-mode (9/125)
fibre length	2.2 km
post-amplifier gain	32 dB
overall gain	0 dB
LD type	DFB

4 Results and discussion

The TD performance (25) is evaluated for different cases, including the RoF system with/without near–far effect by considering the impacts of SF, LF, estimation level and user number. Before considering the near–far effect, the BER performance of the RoF system is evaluated for different OBO values. The results for LF = 100% and SF = 64 are shown in Fig. 3, along with the BER curve (dashed line) corresponding to a linear system, that is, the pure WCDMA system with no optical link. As can be seen, the equalisation technique is able to compensate for the non-linearity except for the 0 dB case (which is never used in practice). To quantify the TD, according to (25) and Fig. 4, the difference in (E_b/N_0) should be computed at a target BER. For the case shown in the figure, the TD at 0 dB is calculated as TD = (3.2) + 0 = 3.2 dB.

4.1 Impact of near–far on TD

To assess the impact of near–far effect on the TD performance of a RoF link, other simulations were carried out for different

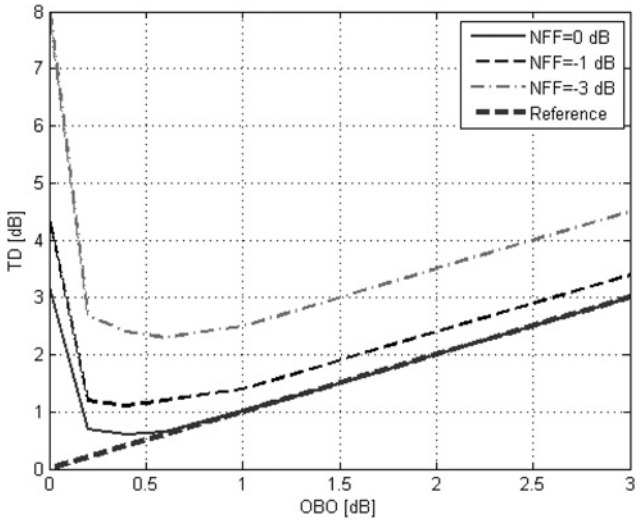

Fig. 4 *TD against E_b/N_0 for DL RoF-WCDMA with near–far effect for user-1*

© The Institution of Engineering and Technology 2014

NFF values. The results for user-1 (the user that transmits/receives the minimum amount of the power) are shown in Fig. 4 for SF = 64 and LF = 100% at frame level estimation. Also, shown in this figure is the TD curve (dashed line) corresponding to a linear system. As can be seen, the optimum TD performance is achieved for small OBO values over the 0.3–0.6 range regardless of NFF values. By referring to Fig. 4 and for such OBO values, it is observed that in the absence of near–far problem, the equalisation technique almost compensates for the non-linearity. In the presence of near–far problem, however, the TD performance is degraded by NFF. For small NFF values (more destructive), say −3 dB, the impact of NFF is too much to be fully compensated by the aforementioned equalisation technique. Nevertheless, for moderate and large NFF values, say −1 dB, the proposed technique can almost accommodate the joint effects of the near–far problem and the non-linearity.

It is worth mentioning that this situation corresponds to the worst-case scenario where the intended user that is, user-1 receives the minimum amount of power. The effect of user number (or alternatively the user location) is discussed in the following subsection. In conclusion, the minimum TD values for three descending values of NFF in dB are 0.6, 1.1 and 2.2, respectively.

4.2 Impact of user number

As discussed in Section 3, the minimum and maximum powers are transmitted/received by user-1 and user-K, respectively. For the NFF = 0 dB case (no near–far effect), the QoS is not different as evidenced before (but not shown). In the presence of near-far, however, the QoS is totally different for different users. For comparison purposes, three users with the maximum power (for $k = K$), minimum power (for $k = 1$) and medium power (for $k \simeq \mathrm{K}/2$) have been selected. The TD results for the worst-case scenario, that is, for NFF = −3 dB are shown in Fig. 5 (left pane) along with the aforementioned reference line for LF = 100 % and SF = 64. As the curves demonstrate, the optimum performance is achieved for the same OBO range (0.3–0.6). Also, a meaningful difference among the TD performances of different users could be observed. Further, the proposed method fully compensates for the non-linearity except for user-1 as the worst case. In summary, the minimum TD values for user-1, user-28 and user-57 in dB are 2.2, 0.8 and 0.3, respectively. To show the eligibility of the proposed method, the same experiment was repeated for NFF = −1 dB. The TD results are shown in Fig. 5 (right pane). As the plots demonstrate, our method can almost compensate for the non-linearity in mild conditions.

4.3 Effect of spreading factor

To assess the impact of the number of users on the system performance (see (15)), two extra values for SF that is, 32 and 128 at a fixed LF value that is, 100% are considered for NFF = −3 dB.

The TD performances for different values of SF are depicted in Fig. 6 for different OBO levels. The TD results show that the performance for SF = 128 is better than the performance for SF = 64 which in turn is better than the performance for SF = 32.

In the linear system, the performance of WCDMA is not changed by SF variations because all the spreading codes, including the pilot signal, are perfectly orthogonal to each other. However, the orthogonality breaks down in the non-linear system which produces MUI. By increasing the number of users for a fixed R, the MUI increases as a result of orthogonality loss between spreading codes. However, the pilot signal of fixed power behaves like a higher power interferer for the desired user as the number of users increases. Hence, the smaller the number of users, the worse the performance. As can be seen, for a fixed OBO level the TD becomes smaller by increasing SF

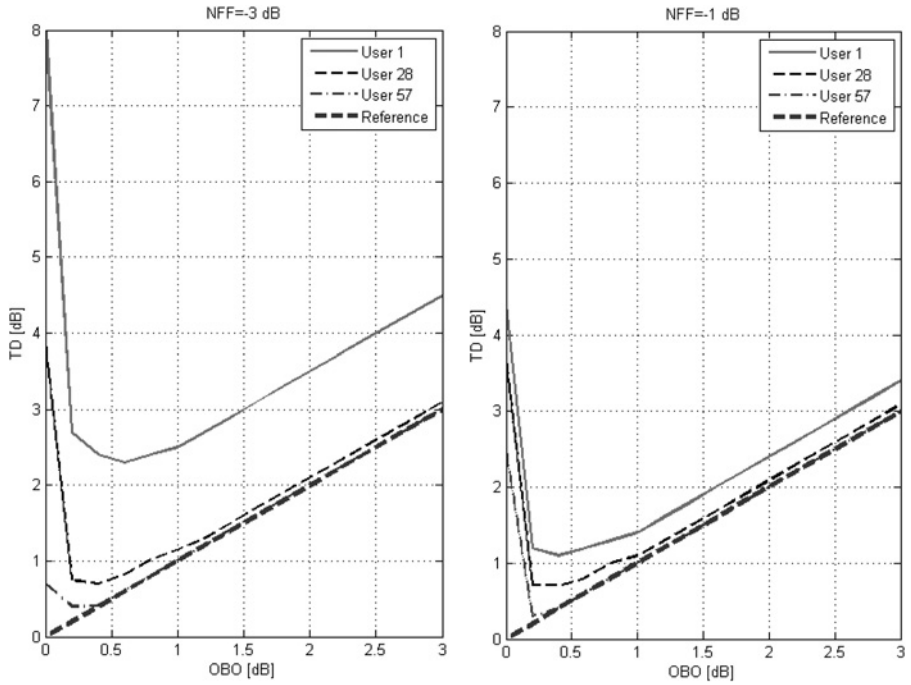

Fig. 5 *TD against E_b/N_0 for DL RoF-WCDMA with near–far effect for NFF = −3 dB (left pane) and NFF = −1 dB (right pane): the effect of user number*

© The Institution of Engineering and Technology 2014

doi: 10.1049/iet-com.2013.0805

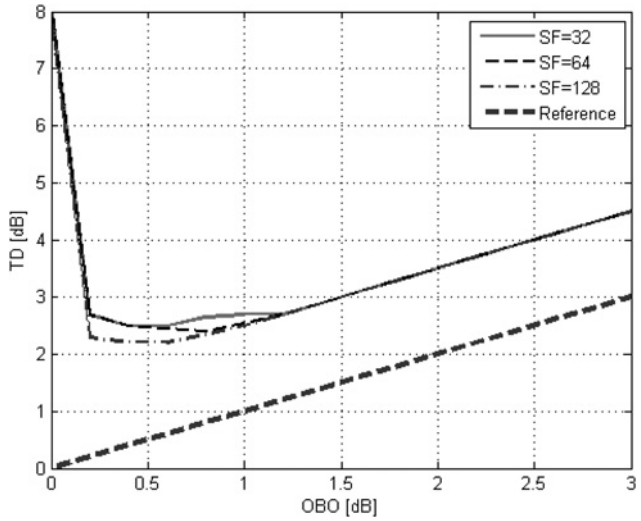

Fig. 6 *TD against E_b/N_0 for DL RoF-WCDMA with near–far effect for user-1: the effect of SF*

(correspondingly by decreasing data rate) which confirms the above analysis. To conclude, the minimum TD values for three ascending values of SF in dB are 2.4, 2.2 and 2.1, respectively.

4.4 Effect of load factor

The effects of load factor (LF) [refer to (15)] on the TD performance of the RoF-WCDMA system are shown in Fig. 7 for the worst-case scenario; that is, user-1 at NFF = −3 dB. Also shown in this figure is the TD curve (dashed line) corresponding to a linear system. In general, by increasing LF the achievable TD performance decreases.

As can be seen, for all values of LF, the curves are tightly packed; that is, the TD is less sensitive to LF. Also, the results indicate that TD plots for large OBO levels are not affected by LF variations. For a fixed R, the number of users (15) increases by increasing LF. Also, the total transmit power P_t is not affected by LF variations. In the non-linear system, the system performance is degraded as a result of loss of orthogonality between the spreading code of the intended user to those of other users as well as that of the pilot signal. By decreasing LF, the number of users decreases, however, the power of each user increases. This means, each other user behaves like a higher power interferer for the desired user. In other words, there is a balance between the number of users and the (interfering) power of each undesired user. In general, LF has a slight effect on the TD performance for all OBO levels. As in the previous case, the optimum performance is achieved for the same OBO range (0.3–0.6).

4.5 Impact of estimation interval

An estimate of the WCDMA channel is obtained by evaluating a portion of the frame over the interval $T_{est} \leq T_{fr}$, which is then applied to whole frame for data recovery. This technique reduces the processing time but the system performance is degraded compared to estimation over a full frame period. In order to investigate the effect of the estimation interval as a new idea on the system performance, the previous experiments were repeated for estimation intervals equal to a slot period ($T_{est} = 0.667$ ms) and a symbol period ($T_{est} = 0.0167$ ms). The corresponding TD curves are plotted in Fig. 8 for the worst-case scenario, that is, user-1 and NFF = −3 dB. As can be seen, by decreasing the estimation interval, the plots demonstrate that the system performance is degraded by decreasing the estimation interval. For the optimum OBO values (0.3–0.6), the TD performances of frame and slot levels are the same, however, that of symbol level is inferior to both of them. In other words, for the same OBO range, the slot level estimation is sufficient for equalisation purposes. Also, the minimum TD values for three estimation intervals from symbol to frame in dB are 3, 2.5 and 2.4, respectively.

The system performance cannot be further improved by the proposed channel estimation technique. Therefore, other techniques such as system equalisation should be used to fully compensate for all impairments. Nonetheless, it should be emphasised that a 0 dB OBO represents a strong non-linearity which is not used in practice; instead the optimum quiescent point is determined by the TD where in this study it is over the 0.3–0.6 interval. The performance of uplink wireless RoF systems is the topic of future investigation by the author.

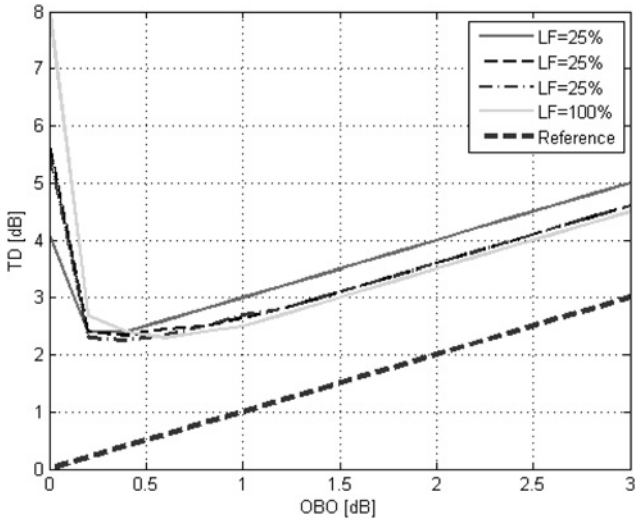

Fig. 7 *TD against E_b/N_0 for DL RoF-WCDMA with near–far effect for user-1: the effect of LF*

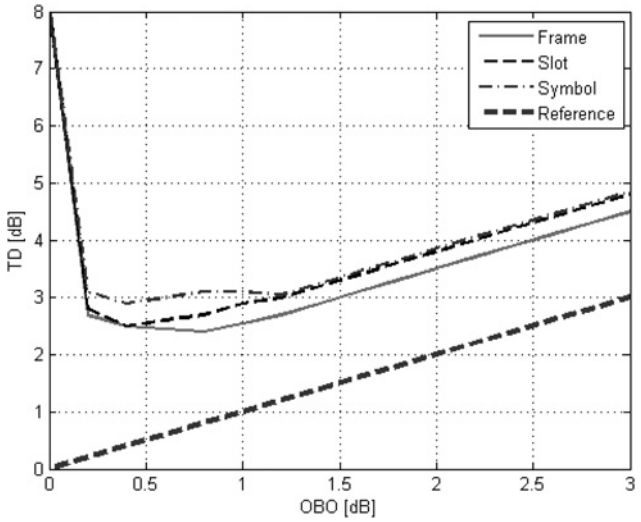

Fig. 8 *TD against E_b/N_0 for DL RoF-WCDMA with near–far effect for user-1: the effect of estimation level*

© The Institution of Engineering and Technology 2014

5 Conclusion

In this paper, the impact of the optical subsystem non-linearities on the system TD performance of a RoF–WCDMA system in the presence of near–far effect for different LFs, SFs, user locations and estimation intervals was investigated. The results demonstrated that pilot-aided channel estimation is an effective technique to equalise a signal degraded by the joint impairments of optical channel and near–far effect. The achievable optimum performance depends on the OBO and NFF values. However, there always exists a value of OBO that minimises the TD performance. In general, by increasing LF and SF, the TD performance was improved. Also, there was a slight decrease in the performance when the channel estimation interval was decreased from a frame to a slot to a symbol interval for the same OBO and NFF values. Further, the QoS can be guaranteed for different users.

6 Acknowledgments

I would like to thank Professor Tim O'Farrell and the anonymous reviewers for their helpful comments that helped to improve this paper considerably.

7 References

1 Baghersalimi, G., O'Farrel, T.: 'Pilot-aided estimation and equalisation of a radio-over-fibre system in wideband code division multiple access', *IET COM*, 2013, **7**, (10), pp. 999–1007
2 Lim, C., Nirmalathas, A., Bakaul, M., *et al.*: 'Fibre-wireless networks and subsystem technologies', *J. Lightw. Technol.*, 2010, **28**, (4), pp. 390–405
3 Develi, I.: 'Application of multilayer perceptron networks to laser diode nonlinearity determination for radio-over-fibre mobile communications', *Microw. Opt. Technol. Lett.*, 2004, **42**, (5), pp. 425–427
4 Yuksel, M.E., Develi, I.: 'A neuro-fuzzy computing technique for modeling laser-diode nonlinearity in a radio-over-fibre link', *Int. J. RF Microw. Comput. Aided Eng.*, 2005, **15**, (3), pp. 329–335
5 Niiho, T., Nakaso, M., Masuda, K., Sasai, H., Utsumi, K., Fuse, M.: 'Transmission performance of multichannel wireless LAN system based on radio-over-fibre techniques', *IEEE Trans. Microw. Theory Tech.*, 2006, **54**, (2), pp. 980–989
6 Yuen, R., Fernando, X.: 'Analysis of sub-carrier multiplexed radio over fibre link for the simultaneous support of WLAN and WCDMA systems', *Wirel. Pers. Commun. Spec. Issue Adv. Wirel. LANs PANs*, 2005, **33**, (1), pp. 1–20
7 Lin, W.P., Peng, W.R., Chi, S.: 'A robust architecture for WDM radio-over-fibre access networks'. Proc. Optical Fibre Communication Conf., 2004, **2**, (3)
8 Fernando, X., Kosek, H., He, Y., Gu, X.: 'Optical domain demultiplexing of subcarrier multiplexed cellular and wireless LAN radio signals'. Proc. SPIE Conf., 2005, pp. 59711S1–59711S10
9 Van Nee, R., Prasad, R.: 'OFDM for wireless multimedia communication' (Artech House, 2000)
10 Goldsmith, A.: 'Wireless communications' (Artech House, 2005)
11 Fernando, X.N., Seasay, A.B.: 'Characteristics of directly modulated RoF Link for wireless access'. CCECE2004, 2004, vol. 4, pp. 2167–2170
12 Baghersalimi, G., O'Farrell, T., Postoyalko, V.: 'Pilot-aided channel estimation in WCDMA on a radio-over-fibre channel'. London Communication Symposium, 2006, pp. 25–28
13 Zhang, J., He, S., Yin, S.: 'A memory polynomial predistorter for compensation of nonlinearity with memory effects in WCDMA transmitter'. ICCCAS, 2009, pp. 913–916
14 Tachikawa, K.: 'W-CDMA mobile communications systems' (Wiley, 2002)
15 Shafinia, M.H., Kabir, P., Pad, P., Mansouri, S.M., Marvasti, F.: 'Errorless codes for CDMA systems with near-far effect'. IEEE ICC, 2010, pp. 1–5
16 Way, W., Afrashteh, A.: 'Linearity characterization of connectorized laser diodes under microwave intensity modulation by am/am and am/pm measurements'. JMTT-S Int. Microwave Symposium Digest, 1986, vol. 86, no. 1, pp. 659–662
17 Bosch, W., Gatti, G.: 'Measurement and simulation of memory effects in pre-distortion linearizers', *IEEE Trans. Microw. Theory Tech.*, 1989, **37**, (12), pp. 1885–1890
18 Lee, C.H.: 'Characterisation and compensation of direct laser modulation nonlinearity in radio-over-fibre systems'. PhD thesis, University of Leeds, 2004
19 Qaraqe, K.A., Roe, S.: 'Channel estimation algorithms for third generation W-CDMA communication systems'. 53rd IEEE Vehicular Technology Conference, 2001, vol. 4, pp. 2675–2679
20 Fazel, K., Kaiser, S.: 'Analysis of non-linear distortions on MC-CDMA'. IEEE Int. Conf. Communications, 1998, vol. 2, pp. 1028–1034
21 3GPP. TS 25.212: Multiplexing and channel coding (FDD), 2006
22 3GPP. TS 25.213: Spreading and modulation (FDD), 2006

© The Institution of Engineering and Technology 2014

doi: 10.1049/iet-com.2013.0805

Copyright of IET Communications is the property of Institution of Engineering & Technology and its content may not be copied or emailed to multiple sites or posted to a listserv without the copyright holder's express written permission. However, users may print, download, or email articles for individual use.